



OPEN ACCESS

EDITED BY

Ayse Peker-Dobie,
Istanbul Technical University, Turkey

REVIEWED BY

Linjie Liu,
Northwest A and F University, China
Umar Farooq,
Abdul Wali Khan University Mardan,
Pakistan

*CORRESPONDENCE

Peiyu Chen,
cpy19@mails.tsinghua.edu.cn

SPECIALTY SECTION

This article was submitted to Social
Physics,
a section of the journal
Frontiers in Physics

RECEIVED 09 June 2022

ACCEPTED 01 July 2022

PUBLISHED 17 August 2022

CITATION

Chen P, Guo X, Jiao Z, Liang S, Li L, Yan J,
Huang Y, Liu Y and Fan W (2022), Effects
of individual heterogeneity and multi-
type information on the coupled
awareness-epidemic dynamics in
multiplex networks.
Front. Phys. 10:964883.
doi: 10.3389/fphy.2022.964883

COPYRIGHT

© 2022 Chen, Guo, Jiao, Liang, Li, Yan,
Huang, Liu and Fan. This is an open-
access article distributed under the
terms of the [Creative Commons
Attribution License \(CC BY\)](#). The use,
distribution or reproduction in other
forums is permitted, provided the
original author(s) and the copyright
owner(s) are credited and that the
original publication in this journal is
cited, in accordance with accepted
academic practice. No use, distribution
or reproduction is permitted which does
not comply with these terms.

Effects of individual heterogeneity and multi-type information on the coupled awareness-epidemic dynamics in multiplex networks

Peiyu Chen^{1*}, Xudong Guo¹, Zengtao Jiao², Shihao Liang²,
Linfeng Li², Jun Yan², Yadong Huang¹, Yi Liu¹ and Wenhui Fan¹

¹Department of automation, Tsinghua University, Beijing, China, ²Yidu Cloud AI Lab, Yidu Cloud (Beijing) Technology Co., Ltd., Beijing, China

Awareness of epidemics can influence people's behavior and further trigger changes in epidemic spreading. Previous studies concentrating on the coupled awareness-epidemic dynamics usually ignore the multi-type information and the heterogeneity of individuals. However, the real-world cases can be more complicated, and the interaction between information diffusion and epidemic spreading needs further study. In this article, we propose an individual-based epidemics and multi-type information spreading (IEMIS) model on two-layered multiplex networks considering positive and negative preventive information and two types of heterogeneity: 1) heterogeneity of aware individual's state which leads to differences in aware transmission capacity and 2) heterogeneity of individual's node degree which affects the epidemic infection rate. Based on Micro-Markov Chain approach (MMCA), we derive the theoretical epidemic threshold for the proposed model and validate the results by those obtained with Monto Carlo (MC) simulations. Through extensive simulations, we demonstrate that for epidemics with low infectivity, promoting the diffusion of positive preventive information, enhancing the importance ratio of neighbors who are aware of positive information, and increasing social distance among individuals can effectively suppress epidemic spreading. However, for highly infectious diseases, the influence of these factors becomes limited.

KEYWORDS

epidemic spreading, information diffusion, multiplex networks, individual heterogeneity, multi-type information

Introduction

Pandemics are major threats to human society Morens et al. [1]. Recently, during the COVID-19 pandemic, epidemic-related information diffused by official media, mass media, or relatives and friends has aroused public awareness. Crisis awareness or negative emotions may propagate among individuals. Such awareness can further influence

people's decision-making or behavior, for e.g., wearing masks, reducing physical contact with others, and receiving the vaccination, and as a result, may trigger changes in epidemic spreading Ferguson [2]; Wang et al. [3]; Funk et al. [4]; Funk et al. [5]; Ruan et al. [6]. Therefore, it is necessary to understand the interaction between information diffusion and epidemic propagation, and this topic has gained much attention in recent studies Arefin et al. [7]; Kabir and Tanimoto [8]; Nadini et al. [9]; Hota and Sundaram [10]; Li and Li [11].

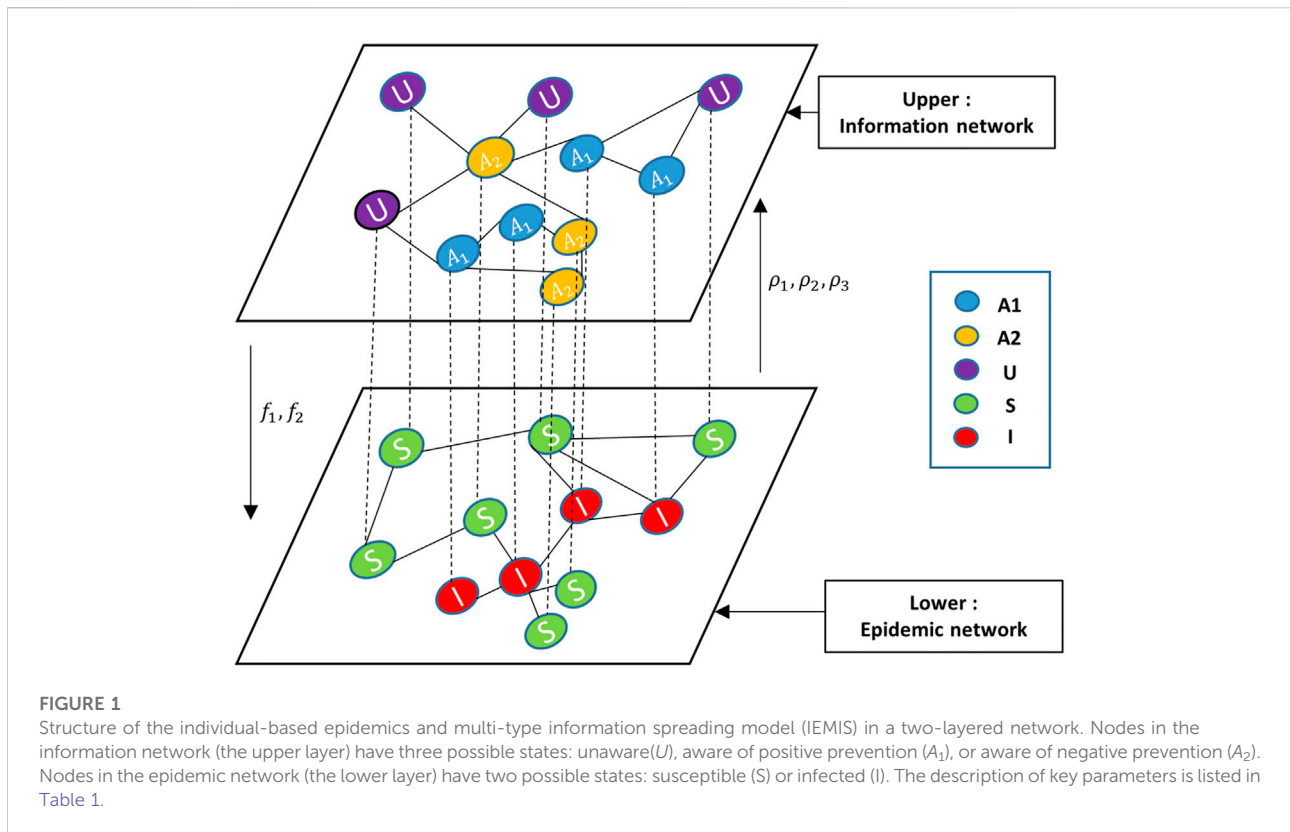
Recent studies on the coupled awareness-epidemic dynamics usually used two asymmetrical networks to represent two spreading processes Wang et al. [12]; Jia et al. [13]; Guo et al. [14]; Zhan et al. [15]; Wang et al. [16], Wang et al. [17]. For example, Kabir et al. [18] constructed a two-layer SIR-UA (susceptible-infected-recovered/unaware-aware) model to study the interaction between physical contact and information diffusion on epidemic spreading. Xia et al. [19] considered the influence of mass media in information diffusion in the awareness-epidemic model and derived the epidemic threshold which is correlated with the multiplex network topology. Guo et al. [20] incorporated three types of heterogeneity with the coupled awareness-epidemic spreading model and pointed out that the heterogeneity has two-stage effects on the epidemic threshold. Li et al. [21] used a temporal multiplex network to study the spatial-temporal properties of multiplex networks to the epidemic spreading. Jia et al. [13] proposed a multi-layer activity-driven network that investigates disease diffusion with self-protection awareness. Their results indicate the impact of network structure and propagation parameters on the epidemic threshold. Kabir et al. [22] presented a susceptible–vaccinated–infected–recovered (SIR/V) with the unaware–aware (UA) epidemic model to study the impact of vaccination on epidemic dynamics. Based on their model, they studied the vaccination game with different types of strategy updating rules and different network topologies.

In the real world, the prevalence of public discussion on epidemics varies and does not always bring about a positive effect on the epidemic spreading Depoux et al. [23]; Ahmad and Murad [24]. For instance, individuals may become vigilant or scared and take protective measures when they receive information regarding the pandemic through official media. That is, a positive correlation between the protective measures taken by individuals and the spread of awareness could be built. However, based on the diversification of information, individuals may be affected by misdirected information regarding the disease spreading on social media and thus become irrational to the epidemic. Irrational behaviors including irrational antimicrobial prescribing Parveen et al. [25], irrational beliefs Teovanovic et al. [26], and panic buying Arafat et al. [27] can facilitate the propagation of epidemics by individuals' improper protective measures. Hence, information diffusion can also lead to a negative correlation between information diffusion and the spread of the epidemic. The issue how the interaction of different types of information influences epidemic propagation

has been further studied. To distinguish the impact of different types of information on disease spread, Zhang et al. [28] introduced a nonlinear dependence of the epidemic infection rate representing the effect of different forms of dependence on the coevolving dynamics. In addition, Wang et al. [29] studied the impact of positive and negative epidemic-related information on disease spread. These studies pointed out the significance of information diversity on the propagation of epidemics. However, assumptions for multiple preventive information are still limited and do not consider the individual heterogeneity in the diffusion of information.

Early studies usually assume that individuals are treated equally, namely, individuals have the same response to epidemics after being aware of the protective measures, and each infected or aware individual has the same influence on their neighbors. In fact, the individual differences lie in its characteristics and relationship with the affected neighbors (e.g., number of contacts, states, and intimacy with infected neighbors) Wang et al. [17]; Liu et al. [30]; Guo et al. [31]; Zhang et al. [32]. For instance, highly connected individuals (hub nodes) have higher infectious rates compared with those lowly connected individuals (weak nodes). In other words, individuals who have large social circles are more likely to affect others or be affected by their neighbors. In recent years, there has been an increasing focus on the study of the influence of individual heterogeneity on epidemic dynamics. Guo et al. [33] described the heterogeneity by using degree and k-core measures in three models based on different assumptions. Results showed a difference in the final epidemic size between the k-core measure and the degree measure. Chen et al. [34] proposed a resource-epidemic co-evolution model in order to study the influence of allocation of individual resources on the dynamic of an epidemic. Also, they came to the conclusion that the heterogeneity of self-awareness distribution suppresses the outbreak of an epidemic. Pan and Yan [35] incorporated the heterogeneity of individual response to disease, the heterogeneity of influence in the epidemic network, and the heterogeneity of influence in the information network in a coupled awareness-epidemic spreading model in multiplex networks. Although studies mentioned previously highlight the necessity of considering individual heterogeneity in the information-epidemic multiplex network-based model, such heterogeneity is simple compared to the reality. Therefore, the issue how individual heterogeneity impacts the interplay between epidemics spreading and awareness diffusion requires further study.

Motivated by the aforementioned considerations, we propose an individual-based epidemics and multi-type information spreading (IEMIS) model upon multiplex networks. To investigate the impact of multi-type information, we introduce two types of information: 1) positive and 2) negative preventive information. The diffusion of awareness can reduce or increase the risk of infection depending on its type. Considering that the



diffusion speed of awareness is also related to the information type and the epidemic dynamics, the transmission rate of different types of information varies. Moreover, to explore the influence of individual heterogeneity on the interaction between information and disease, two types of heterogeneity are considered: 1) heterogeneity of aware individuals' states (health state and information type) which contributes to different aware transmission capacities and 2) heterogeneity of individual's node degree which influences the epidemic infection rate. In this study, we aim to answer the following questions: 1) how do two classes of information affect epidemic spreading when considering individual heterogeneity? 2) how do the two types of individual heterogeneity affect epidemic spreading? and 3) how do the other disease-related or information-related parameters influence the individual heterogeneity?

The remainder of this article is organized as follows. In Section 2, we describe the individual-based epidemics and multi-type information spreading model. In Section 3, we analyze the proposed model by MMCA and derive the analytical expression of the epidemic threshold. In Section 4, we compare the results simulated by MMC and MC methods, validate the accuracy of the MMC method, and investigate the impact of different types of information and individual heterogeneity. In Section 5, we present some concluding remarks for our findings.

Model description

In this article, we proposed an individual-based epidemics and multi-type information spreading model (IEMIS) by two-layered multiplex networks, as presented in Figure 1. The upper layer represents the information diffusion based on the information network, where links represent connections with information spreaders such as friends on Twitter or Facebook, while the lower layer supports the propagation of epidemics, where links denote physical contacts among individuals, e.g., contacts among family members, classmates, or colleagues. Each layer can be represented as a graph $G = (V, E)$, where V and E denote individuals and their links, respectively. The link set X and Y represent the adjacency matrices of epidemic and information networks. The description of key parameters is listed in Table 1. The interactions between the two processes and the corresponding propagation regulations are as follows:

Propagation rules

1. Information diffusion. In the upper layer, nodes are separated into three types: unaware (U), aware of positive prevention (A_1), and aware of negative prevention (A_2). Individuals in state U do not have any awareness about the epidemic

TABLE 1 Definitions of key parameters.

Parameter	Description
β	Probability of getting infected by infected neighbors for susceptible individuals
μ	Probability of being recovered for infected individuals
δ_1	Probability of being unaware of disease for A_1S
δ_2	Probability of being unaware of disease for A_2S
λ_1	Probability of being aware of positive information for US
λ_2	Probability of being aware of negative information for US
f_1	Positive awareness perception factor
f_2	Negative awareness perception factor
$\rho_1, \rho_2,$ and ρ_3	Health-related factors for aware neighbors to spread awareness
$1 - e^{-k_j/\sum k}$	Node degree-related factors for infected neighbors to spread disease

prevention. Here, individuals in A_1 and A_2 are both aware of the disease but take different precautions toward the disease. Individuals in state A_1 can take effective precautions toward the disease and have lower infection rates than unaware individuals. On the contrary, individuals in state A_2 tend to take irrational preventive measures which lead to higher infection rates than unaware individuals. The unaware individuals can get awareness through contact with neighbors in state A_1 (A_2) with probability λ_1 (λ_2). Also, individuals in state A_1 and A_2 may forget the awareness with probabilities δ_1 and δ_2 , respectively. Moreover, in terms of the awareness-related impact on the epidemic spreading, susceptible individuals whose states are A_1 and A_2 can influence the probability of being infected by multiplication factors f_1 ($0 \leq f_1 \leq 1$) and f_2 ($1 \leq f_2 \leq 2$), respectively. The lower the multiplication factor is, the lower the probability of individuals being infected is, especially when $f_1 = 0$, individuals are fully immune to the infectious disease.

2. Epidemic propagation. In the lower layer, there exist two different health-related states: susceptible(S) and infected (I). Susceptible individuals may be infected with the probability β by infected (I) neighbors when they are unaware of epidemics. The susceptible individuals who are in state A_1 and A_2 may be infected with probabilities $f_1\beta$ and $f_2\beta$, respectively. Also, the infected (I) individuals recover with the probability of μ .
3. Heterogeneity of aware individuals' states. Aware individuals in different states (health state and information type) have different aware transmission capacities. It is known that, in many cases, awareness spread by infected individuals can be more persuasive than healthy people. Neighbors of those infected individuals tend to be more alert to the infectious disease and more willing to take protective measures. In addition, individuals in A_1 and A_2 states also play different roles in awareness diffusion. We assume that unaware people are more likely to acquire positive preventive information rather than the negative one. Compared with the former

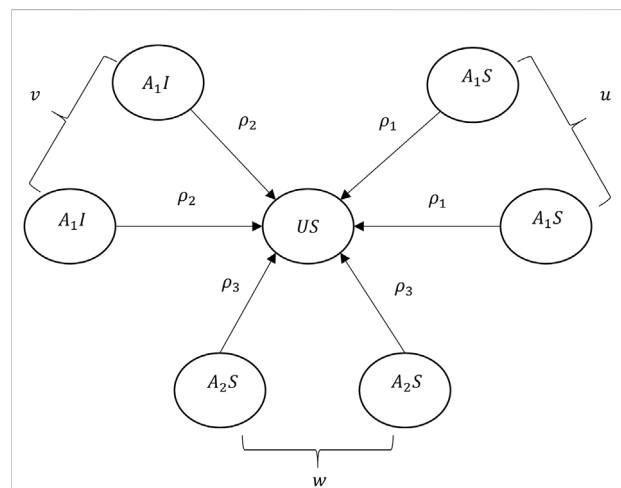
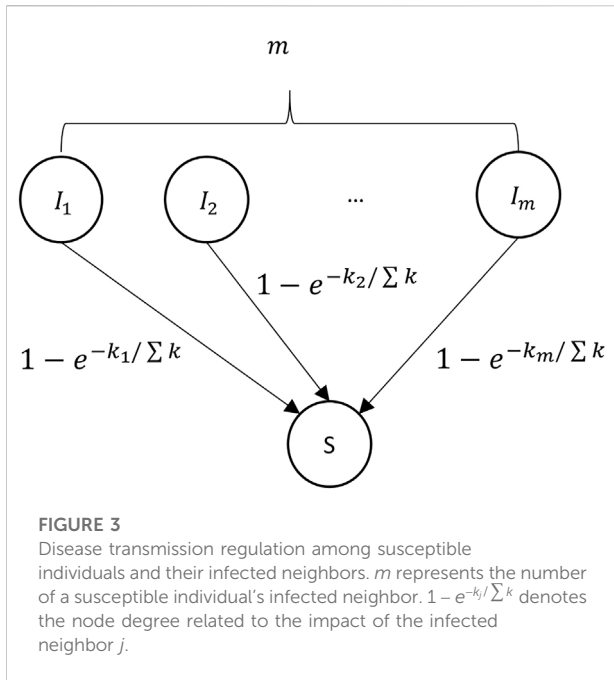


FIGURE 2 Sketch map of the awareness diffusion between unaware individuals and their aware neighbors. $u, v,$ and w denote the number of $A_1S, A_1I,$ and $A_2S,$ respectively. $\rho_1, \rho_2,$ and ρ_3 are the health-related factors.

studies Wang et al. [29], Wang et al. [17], which assume that aware neighbors have the same contribution on awareness spreading (important ratio of aware individuals $A_1S : A_1I : A_2S = \frac{1}{3} : \frac{1}{3} : \frac{1}{3}$), we believe that aware neighbors have different importance ratios based on their state $A_1S : A_1I : A_2S = \frac{1}{3} + \Delta\rho_1 : \frac{1}{3} + \Delta\rho_2 : \frac{1}{3} + \Delta\rho_3 = \rho_1 : \rho_2 : \rho_3 (\Delta\rho_1 + \Delta\rho_2 + \Delta\rho_3 = 0)$. $\rho_1, \rho_2,$ and ρ_3 are the health-related factors that represent different importance ratios of awareness spreading for individual in different states. Figure 2 presents a sketch map of the awareness diffusion between an unaware individual and its aware neighbors.

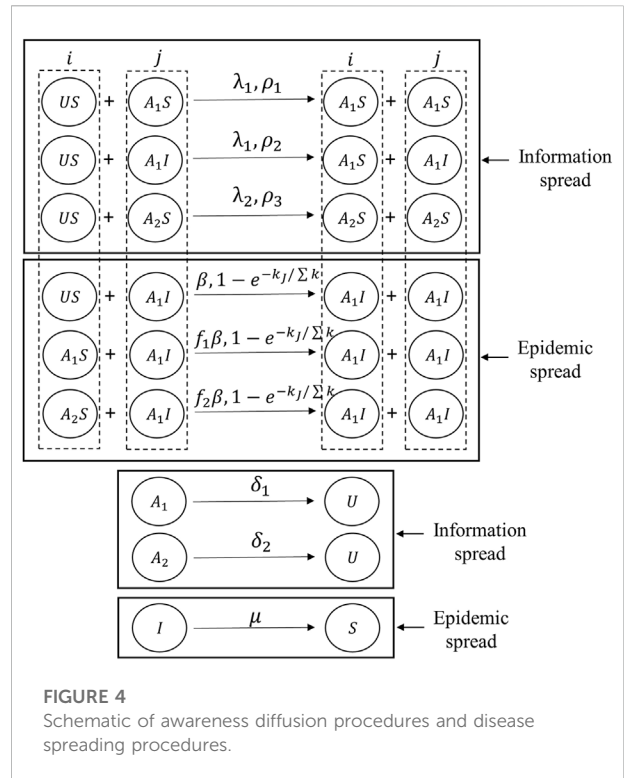
4. Heterogeneity of individual's node degree. The degree distribution of the epidemic network contributes to the heterogeneity of infection rate for susceptible individuals.



The infected individuals with a large node degree mean that they have frequent social activities and are highly connected with their neighbors. Such hub nodes are more likely to be the virus carrier. Hence, the node degree k_i is used to represent the impact of infected node i , and $k_i/\sum k$ is regarded as the influence weight where $\sum k$ is the total degree of the infected neighbors. Figure 3 shows the disease transmission regulation between a susceptible individual and its infected neighbors. Here, $1 - e^{-k_i/\sum k}$ quantifies the probability of being infected by the infected neighbor i .

Awareness-epidemic-based dynamics

Here, we assume that once an individual is infected, the individual would be aware of the positive preventive information. Considering the combination of health states and awareness states, there are four possible states in our model: 1) US (susceptible individual who is unaware of epidemic), 2) A_1S (susceptible individual who is aware of positive preventive information), 3) A_2S (susceptible individual who is aware of negative preventive information), and (4) A_1I (infected individual who is aware of positive preventive information). The possible state transition procedures are presented in Figure 4. It should be noted that Figure 4 only indicates the state transitions of individual i by its neighbor j who has a transmission capacity of disease or information after a possible epidemic or information spread. That is, Figure 4 only presents changes in the state of individual i . Also, it does not denote a transition



in a time step for both the state in epidemic, and information networks of individual i would change in a time step. For example, a susceptible individual who is unaware of the epidemic (US) would be informed by its neighbor j who is in state A_1S with a certain probability related to λ_1 and ρ_1 . In addition, we assume that in the upper layer once the unaware individual receives a certain kind of information, the individual will not be able to accept other information at this time step.

Analytical results based on MMCA

In this section, the proposed epidemic model is analyzed, and the epidemic threshold β_c is given by MMCA. The probabilities that one individual be in one of the four states at time t can be given as $P_i^{US}(t)$, $P_i^{A_1S}(t)$, $P_i^{A_2S}(t)$, and $P_i^{A_1I}(t)$, respectively. Restriction $P_i^{US}(t) + P_i^{A_1S}(t) + P_i^{A_2S}(t) + P_i^{A_1I}(t) = 1$ should be satisfied at each time step t .

Let x_{ij} and y_{ij} be the adjacency matrices of the epidemic and information network, respectively. If a link exists between nodes i and j in the epidemic (information) network, then x_{ij} (y_{ij}) = 1. Otherwise, x_{ij} (y_{ij}) = 0. Assuming that the possibilities of becoming infected or aware by neighbors are independent, we define the probability of individual i not being aware of positive or negative information at time t by $r_{i1}(t)$ and $r_{i2}(t)$. In addition, q_1^U is denoted as the probability that the susceptible

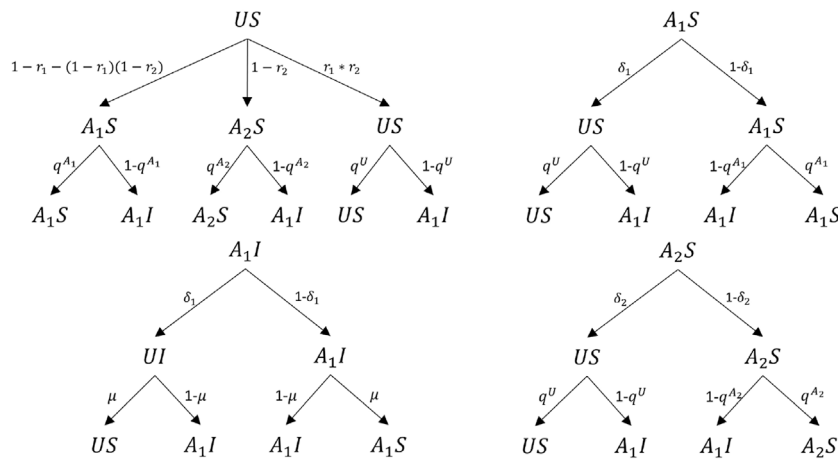


FIGURE 5
Transition probability trees for four states (US, A₁S, A₂S, A₁I).

individual who is not aware of the infectious disease will not be infected at time t . Similarly, $q_I^{A_1}$ ($q_I^{A_2}$) is denoted as the probability that the susceptible individual who is aware of the infectious disease by positive (negative) information will not be infected at time t . The expressions for $r_{i1}(t)$, $r_{i1}(t)$, q_I^U , $q_I^{A_1}$, and $q_I^{A_2}$ are as follows:

$$\left\{ \begin{array}{l} r_{i1}(t) = \prod_u [1 - x_{ui} P_u^{A_1S}(t) \lambda_1]^{p_1} * \\ \prod_v [1 - x_{vi} P_v^{A_1I}(t) \lambda_1]^{p_2} \\ r_{i2}(t) = \prod_w [1 - x_{wi} P_w^{A_2S}(t) \lambda_2]^{p_3} \\ q_I^{A_1}(t) = \prod_j [1 - y_{ij} P_j^{A_1I}(t) f_1 \beta]^{1 + \left(\frac{1 - e^{-k_j}}{\sum k} \right)} \\ q_I^{A_2}(t) = \prod_j [1 - y_{ij} P_j^{A_1I}(t) f_2 \beta]^{1 + \left(\frac{1 - e^{-k_j}}{\sum k} \right)} \\ q_I^U(t) = \prod_j [1 - y_{ij} P_j^{A_1I}(t) \beta]^{1 + \left(\frac{1 - e^{-k_j}}{\sum k} \right)} \end{array} \right. \quad (1)$$

Here, u represents the number of neighbors of individual i in state A_1S , v represents the number of neighbors in state A_1I , and w represents the number of neighbors in state A_2S . Based on the definition of each state, transition probability trees for the four states (US, A₁S, A₂S, A₁I) are presented in Figure 5. As shown in Figure 5, each individual will transmit its states according to the transition trees and its current state in each time step. Individuals who are aware of the positive (negative) information tend to forget the information with probability δ_1 (δ_2). μ denotes the probability of being recovered for an infected individual. According to the transition trees, transition equations for individual i by using MMCA are listed in Eq (2):

$$\left\{ \begin{array}{l} P_i^{US}(t+1) = P_i^{A_1S}(t) \delta_1 q_I^U(t) + P_i^{A_2S}(t) \delta_2 q_I^U(t) + P_i^{US}(t) r_{i1}(t) r_{i2}(t) q_I^U(t) \\ P_i^{A_1I}(t+1) = P_i^{A_1S}(t) \{ \delta_1 [1 - q_I^U(t)] + (1 - \delta_1) [1 - q_I^{A_1}(t)] \} + P_i^{A_2S}(t) \{ \delta_2 [1 - q_I^U(t)] + \\ (1 - \delta_2) [1 - q_I^{A_2}(t)] \} + P_i^{US}(t) \{ r_{i1}(t) r_{i2}(t) [1 - q_I^U(t)] + \\ [1 - r_{i1}(t) - (1 - r_{i1}(t)) (1 - r_{i2}(t))] [1 - q_I^{A_1}(t)] + \\ [1 - r_{i2}(t)] [1 - q_I^{A_2}(t)] \} + P_i^{A_1I}(t) (1 - \mu) \\ P_i^{A_1S}(t+1) = P_i^{A_1S}(t) (1 - \delta_1) q_I^{A_1}(t) + P_i^{A_1I}(t) (1 - \delta_1) \mu + \\ P_i^{US}(t) [1 - r_{i1}(t) - (1 - r_{i1}(t)) (1 - r_{i2}(t))] q_I^{A_1}(t) \\ P_i^{A_2S}(t+1) = P_i^{A_2S}(t) (1 - \delta_2) q_I^{A_2}(t) + P_i^{US}(t) [1 - r_{i2}(t)] q_I^{A_2}(t) \end{array} \right. \quad (2)$$

where $P_i^{US}(t+1)$, $P_i^{A_1I}(t+1)$, $P_i^{A_1S}(t+1)$ and $P_i^{A_2S}(t+1)$ represent the possibility that individual i will be in states US, A₁I, A₁S, and A₂S at the next time step.

When $t \rightarrow \infty$, the model will lead to a steady state and the probabilities for individuals being in each state will be fixed. The solution for Eq 2 should satisfy the following equations:

$$\left\{ \begin{array}{l} P_i^{US}(t+1) = P_i^{US}(t) = P_i^{US} \\ P_i^{A_1I}(t+1) = P_i^{A_1I}(t) = P_i^{A_1I} \\ P_i^{A_1S}(t+1) = P_i^{A_1S}(t) = P_i^{A_1S} \\ P_i^{A_2S}(t+1) = P_i^{A_2S}(t) = P_i^{A_2S} \end{array} \right. \quad (3)$$

where P_i^{US} , $P_i^{A_1I}$, $P_i^{A_1S}$ and $P_i^{A_2S}$ represent the probabilities of an individual to be in states US, A₁I, A₁S, and A₂S at the steady state. In terms of an SIS epidemic model, the number of infected individuals would be next to nil at the steady state when β is close to β_c ; otherwise, the infectious disease transmission will persist in the population for some time. Hence, we assume that $P_i^{A_1I} = \epsilon_i \ll 1$. Also, the high-order terms in Eq 1 can be ignored, and the approximation of $q_i^{A_1}$, $q_i^{A_2}$ and q_i^U can be expressed as:

$$\left\{ \begin{array}{l} q_i^{A_1} \approx 1 - f_1 \beta \sum_j \left(2 - e^{-k_j} / \sum k \right) y_{ij} \epsilon_j \\ q_i^{A_2} \approx 1 - f_2 \beta \sum_j \left(2 - e^{-k_j} / \sum k \right) y_{ij} \epsilon_j \\ q_i^U \approx 1 - \beta \sum_j \left(2 - e^{-k_j} / \sum k \right) y_{ij} \epsilon_j \end{array} \right. \quad (4)$$

We define Eq 5 to simplify Eq 2. Here, $q_i^{A_1} \approx 1 - \alpha_i^{A_1}$, $q_i^{A_2} \approx 1 - \alpha_i^{A_2}$, and $q_i^U \approx 1 - \alpha_i^U$. Eq 2 can further be transformed as Eq 6:

$$\begin{cases} \alpha_i^{A_1} = f_1 \beta \sum_j \left(2 - e^{-k_j} / \sum^k \right) y_{ij} \varepsilon_j \\ \alpha_i^{A_2} = f_2 \beta \sum_j \left(2 - e^{-k_j} / \sum^k \right) y_{ij} \varepsilon_j \\ \alpha_i^U = \beta \sum_j \left(2 - e^{-k_j} / \sum^k \right) y_{ij} \varepsilon_j \end{cases} \quad (5)$$

Ignoring the high-order items, Eq 6 can further be transformed into Eq 7:

$$\begin{cases} P_i^{US} = P_i^{A_1S} \delta_1 (1 - \alpha_i^U) + P_i^{A_2S} \delta_2 (1 - \alpha_i^U) + P_i^{US} r_{11} r_{12} (1 - \alpha_i^U) \\ P_i^{A_1I} = P_i^{A_1S} [\delta_1 \alpha_i^U + (1 - \delta_1) \alpha_i^{A_1}] + P_i^{A_2S} [\delta_2 \alpha_i^U + (1 - \delta_2) \alpha_i^{A_2}] \\ + P_i^{US} [r_{11} r_{12} \alpha_i^U + (r_{12} - r_{11} r_{12}) \alpha_i^{A_1} + (1 - r_{12}) \alpha_i^{A_2}] + P_i^{A_1I} (1 - \mu), P_i^{A_1S} \\ = P_i^{A_1S} (1 - \delta_1) (1 - \alpha_i^{A_1}) + P_i^{A_1I} (1 - \delta_1) \mu + P_i^{US} (r_{12} - r_{11} r_{12}) (1 - \alpha_i^{A_1}), P_i^{A_2S} \\ = P_i^{A_2S} (1 - \delta_2) (1 - \alpha_i^{A_2}) + P_i^{US} (1 - r_{12}) (1 - \alpha_i^{A_2}), \\ \left\{ \begin{array}{l} P_i^{US} = P_i^{A_1S} \delta_1 + P_i^{A_2S} \delta_2 + P_i^{US} r_{11} r_{12} \\ P_i^{A_1S} = P_i^{A_1S} (1 - \delta_1) + P_i^{A_1I} (1 - \delta_1) \mu + P_i^{US} (r_{12} - r_{11} r_{12}) \\ P_i^{A_2S} = P_i^{A_2S} (1 - \delta_2) + P_i^{US} (1 - r_{12}) \\ \varepsilon_i = P_i^{A_1S} [\delta_1 \alpha_i^U + (1 - \delta_1) \alpha_i^{A_1}] + P_i^{A_2S} [\delta_2 \alpha_i^U + (1 - \delta_2) \alpha_i^{A_2}] \\ + P_i^{US} [r_{11} r_{12} \alpha_i^U + (r_{12} - r_{11} r_{12}) \alpha_i^{A_1} + (1 - r_{12}) \alpha_i^{A_2}] \\ + \varepsilon_i (1 - \mu) \end{array} \right. \quad (7)$$

Eq 7 can further be reduced to Eq 8 by substituting the first three equations into the fourth one. At the steady state, we assume that $P_i^{A_1S} + P_i^{A_1I} = P_i^{A_1}$, $P_i^{A_2S} = P_i^{A_2}$. Owing to $P_i^{A_1I} = \varepsilon_i \ll 1$, $P_i^{A_1S} + P_i^{A_2S} \approx P_i^{A_1} + P_i^{A_2}$, and $P_i^{US} \approx 1 - (P_i^{A_1} + P_i^{A_2})$. Then, substituting the aforementioned equations into Eq 8, we get Equation 9:

$$\begin{cases} \mu \varepsilon_i = P_i^{A_1S} \alpha_i^{A_1} + P_i^{A_2S} \alpha_i^{A_2} + P_i^{US} \alpha_i^U \\ = P_i^{A_1S} f_1 \beta \sum_j \left(2 - e^{-k_j} / \sum^k \right) y_{ij} \varepsilon_j + \\ P_i^{A_2S} f_2 \beta \sum_j \left(2 - e^{-k_j} / \sum^k \right) y_{ij} \varepsilon_j + \\ P_i^{US} \beta \sum_j \left(2 - e^{-k_j} / \sum^k \right) y_{ij} \varepsilon_j \\ = (P_i^{A_1S} f_1 + P_i^{A_2S} f_2 + P_i^{US}) \beta \sum_j \left(2 - e^{-k_j} / \sum^k \right) y_{ij} \varepsilon_j \end{cases}, \quad (8)$$

$$\sum_j \left\{ \left[1 - (1 - f_1) P_i^{A_1} - (1 - f_2) P_i^{A_2} \right] \left(2 - e^{-k_j} / \sum^k \right) y_{ji} - \frac{\mu}{\beta} \tau_{ij} \right\} \varepsilon_j = 0. \quad (9)$$

Here, τ_{ij} is the element of the identity matrix. We define a matrix H whose element is $h_{ij} = [1 - (1 - f_1) P_i^{A_1} - (1 - f_2) P_i^{A_2}] (2 - e^{-k_j} / \sum^k) y_{ji} - \frac{\mu}{\beta} \tau_{ij}$. $\Lambda_{\max}(H)$ denotes the maximum eigenvalue of H . The epidemic threshold

β_c is the minimum value of β that satisfies Eq 9. The expression of epidemic threshold β_c is

$$\beta_c = \frac{\mu}{\Lambda_{\max}(H)}. \quad (10)$$

Eq 10 shows that the epidemic threshold is related to the recovery rate μ , the positive (negative) awareness perception factor f_1 (f_2), and the probability of being in state A_1 (A_2). It should be noted that $P_i^{A_1}$ and $P_i^{A_2}$ are further determined by the epidemic-related parameters (epidemic network structure, epidemic transmission rate λ_1 , λ_2 , and recovery rate μ).

Results

In this section, we apply the MMCA and the MC method to analyze the interaction between information diffusion and disease spreading Lyubartsev et al. [36]. For the results of MMCA, the stationary fraction of individuals in states I , A_1 , and A_2 are calculated as $\rho^I = \sum_i P_i^{A_1I} / N$, $\rho^{A_1} = [\sum_i (P_i^{A_1I} + P_i^{A_1S})] / N$, and $\rho^{A_2} = \sum_i P_i^{A_2S} / N$, where N is the total number of nodes and $P_i^{A_1I}$, $P_i^{A_1S}$, and $P_i^{A_2S}$ are the probabilities that node i is at the state A_1I , A_1S , and A_2S , respectively. Also, for the results of MC simulations, $\rho^I = N_{A_1I} / N$, $\rho^{A_1} = (N_{A_1I} + N_{A_1S}) / N$, and $\rho^{A_2} = N_{A_2S} / N$, where N_{A_1I} , N_{A_1S} , and N_{A_2S} denotes the number of nodes in A_1I , A_1S , and A_2S , respectively. The simulation results are based on 30 independent realizations with 1,000 nodes ($N = 1,000$). The information network is generated with the Erdős–Rényi (ER) model Erdős and Rényi [37] with an average degree of 5, while the epidemic network is created with the *BarabásiAlbert* (BA) scale-free model Barabasi and Albert [38] which starts from 5 connected nodes. The number of new edges for a new node added to the existing nodes is 5. The initial fraction of ρ^I , ρ^{A_1} , and ρ^{A_2} is set to be 0.01. The default values of parameters are set to be $\beta = 0.3$, $\mu = 0.5$, $\lambda_1 = \lambda_2 = 0.6$, $\delta_1 = \delta_2 = 0.3$, $f_1 = 0.9$, $f_2 = 1.1$, $\rho_1 = 0.7337$, $\rho_2 = 1.3557$, $\rho_3 = 0.9107$ (Supplementary material Table S1). We analyze the impact of information diversity and different types of heterogeneity on the awareness-epidemic multiple networks through the statistical results of ρ^{A_1I} , ρ^{A_1S} , ρ^{A_1} , and β_c . It should be noted that the proportion of ρ^{A_2S} is not studied in our work for it reaches 0 at the steady state. This can be attributed to our model assumption that people are more willing to receive positive awareness and people being infected can also be aware of positive information.

We first test the accuracy of MMCA in solving our proposed model by comparing the output with the result of the MC method. Then, we study the impact of multi-type information, heterogeneity of aware individuals' states, and heterogeneity of individual's node degree, respectively. Also, the parameters mentioned in the following sections are all used for illustration.

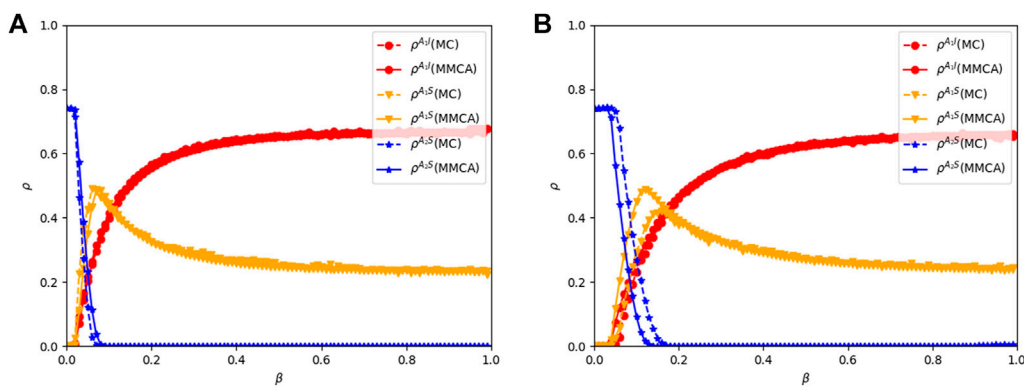


FIGURE 6

Comparison between MMCA and MC simulation. Result shows the proportions of ρ^{A1I} , ρ^{A1S} , and ρ^{A2S} with the increase of β . (A) Networks in the information and physical layers are the BA and ER networks, respectively. (B) Networks in the information and physical layers are both ER networks. All results are averaged by 50 realizations.

Model validation and the impact of β

Figure 6 presents comparisons between MMCA and MC simulation under different network structures. It shows the proportions of ρ^{A1I} , ρ^{A1S} , and ρ^{A2S} by MMCA and MC simulation as functions of the probability of being infected (β). As a result, a good agreement between the two methods can be seen, verifying the accuracy of MMCA used in our awareness-disease multiplex networks. Considering the impact of infection rate β , the tendency of the curves can be divided into three phases. When β is lower than β_c (first phase), few infections would be witnessed and the disease would not be spread to a wide range. With the increase of β (second phase), the proportion of infectious disease (ρ^I) and the positive awareness (ρ^{A1S}) grow vigorously, while the proportion of negative awareness (ρ^{A2S}) falls. This can be explained by the fact that with the increase of infections, the number of positive awareness spreaders increases, holding back the spread of negative awareness. In other words, people would raise their vigilance toward disease and tend to take more preventive measures when the epidemic becomes serious. However, after ρ^{A2S} reduces to 0, ρ^{A1S} also decreases with the increase of β . This is attributed to the individuals' state transition from $A1S$ to $A1I$. In reality, due to the limited protective capability that preventive measures can provide, people would be vulnerable to infectious disease when the infection rate is too high.

In addition, the epidemic is more possible to outbreak in the BA-ER networks comparing the epidemic threshold (β_c) between Figures 6A, B. However, the difference between the results of two network structures decreases with the increase of β . The comparisons indicate that the structure of the multiplex network influences the final epidemic size but can be negligible when the infectious rate (β) is large, playing a dominant role in the dynamic of awareness-disease spreading.

Impact of multi-type information

Considering the impact of information diversity on the epidemic spreading, f_1 , f_2 , λ_1 , and λ_2 are studied in this section, especially f_1 and f_2 denote the degree of influence of positive or negative information on epidemic spreading, respectively, while λ_1 and λ_2 represent the probability of positive or negative information diffusion. To investigate the role of f_1 and f_2 , Figure 7 presents the heat map of the proportions of ρ^{A1I} and ρ^{A1S} by MMCA and MC simulation with a wide range of f_1 and f_2 , while Figure 9 shows the proportions of ρ^{A1} (a) and β_c (b) by MMCA as functions of f_1 and f_2 . Results in Figures 7A, B are obtained by the MC method, and results in Figures 7C, D are obtained by MMCA. It is shown that the results obtained by MMCA are well agreed with the results obtained by MC simulation. Results of Figures 7C, D show that the proportions of ρ^{A1I} and ρ^{A1S} are more sensitive to the variation of f_1 than f_2 . This can be interpreted by the fact that the proportion of ρ^{A2S} is small, and the negative awareness does not play a dominant role in the epidemic spreading. As for f_1 , decreasing f_1 can effectively suppress the spread of disease (ρ^{A1I} decreases with the decrease of f_1 in Figure C). That is, expanding the influence of positive awareness on epidemic spreading can help reducing the final epidemic size. Moreover, for a fixed $f_1 \leq 0.4$, there is an obvious decrease in ρ^{A1I} . When $f_1 \geq 0.4$, a slowdown in the decrease of epidemic size can be seen. The result indicates that the positive awareness should be effective enough to suppress the disease spreading; otherwise, the awareness diffusion would play a little role in epidemic spreading.

Figure 7E presents the impact of f_1 on the awareness spreading. When $f_1 \leq 0.2$, ρ^{A1} increases as f_1 decreases. When $f_1 \geq 0.2$, ρ^{A1} decreases as f_1 decreases. ρ^{A1} reaches a maximum when $f_1 = 0.2$ approximately. This phenomenon can be contributed to the interplay between disease spreading and awareness diffusion. The variation of f_1 affects the dynamic of awareness-epidemic spreading in two ways: (a) the infection

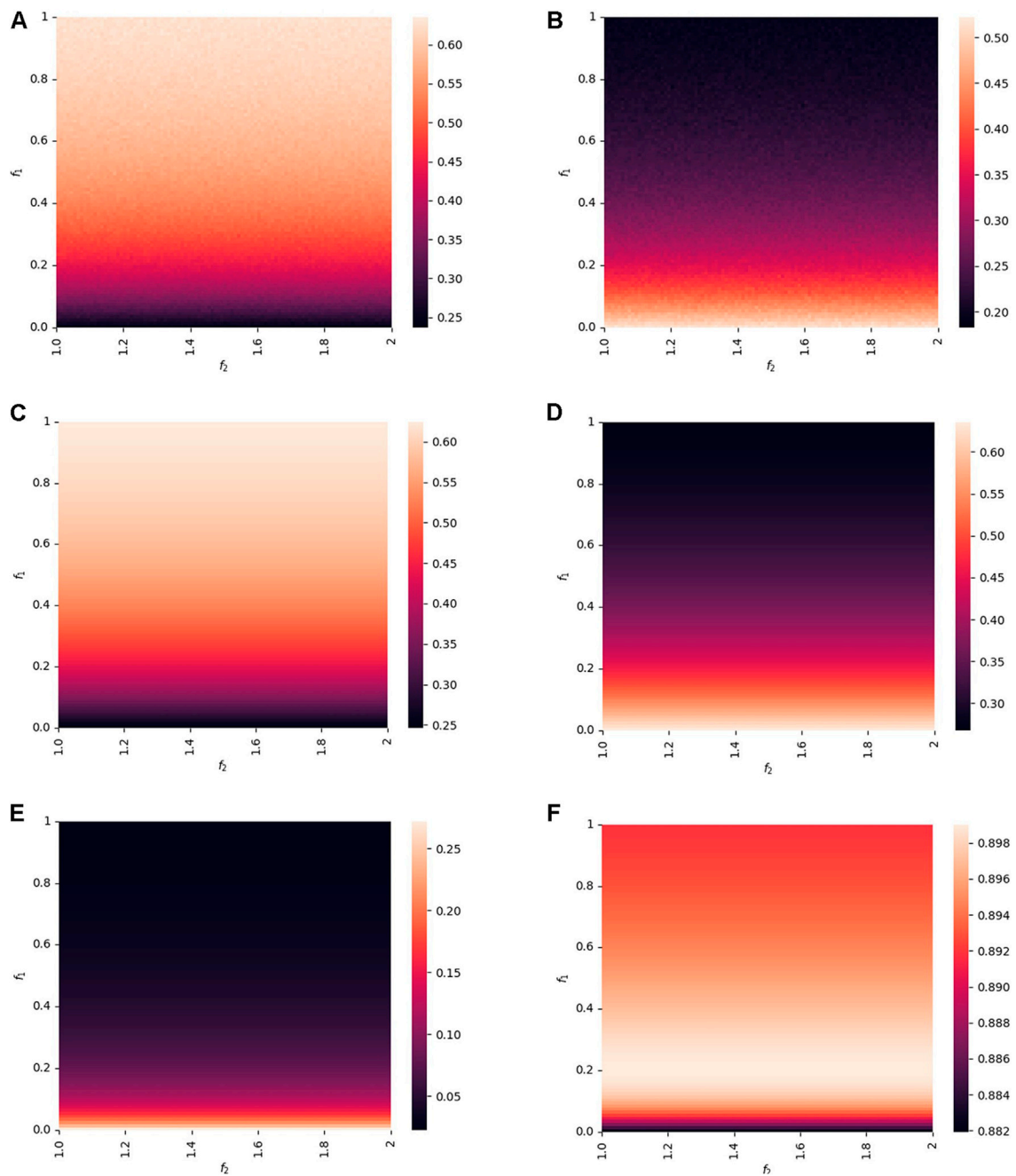


FIGURE 7 Proportions of ρ^{A1I} and ρ^{A1S} by MMCA and MC simulation as functions of f_1 and f_2 (the positive and negative awareness perception, respectively.) The proportions get larger when the color varies from dark to light. Each heat map consists of 100×100 lattice points. (A,C) ρ^{A1I} obtained by MC simulation and MMCA, respectively. (B,D) ρ^{A1S} obtained by MC simulation and MMCA, respectively. (E,F) ρ^{A1} and β_c obtained by MMCA. Other parameters are the same as the default values.

probability increases with the increase of f_1 and promotes the epidemic spreading. (b) The increase of f_1 also accelerates the spread of positive awareness for those being infected; they will automatically become aware of positive information and hold up the disease spreading in turn. Hence, when f_1 is at a low level

($f_1 \leq 0.2$), the diffusion of positive awareness plays a dominant role in the awareness-disease spreading dynamic and contributes to the decrease of ρ^{A1I} . Otherwise, when f_1 is at a high level ($f_1 \geq 0.2$), the effect of promoting awareness diffusion is overwhelmed by the influence of promoting epidemic spreading, leading to an

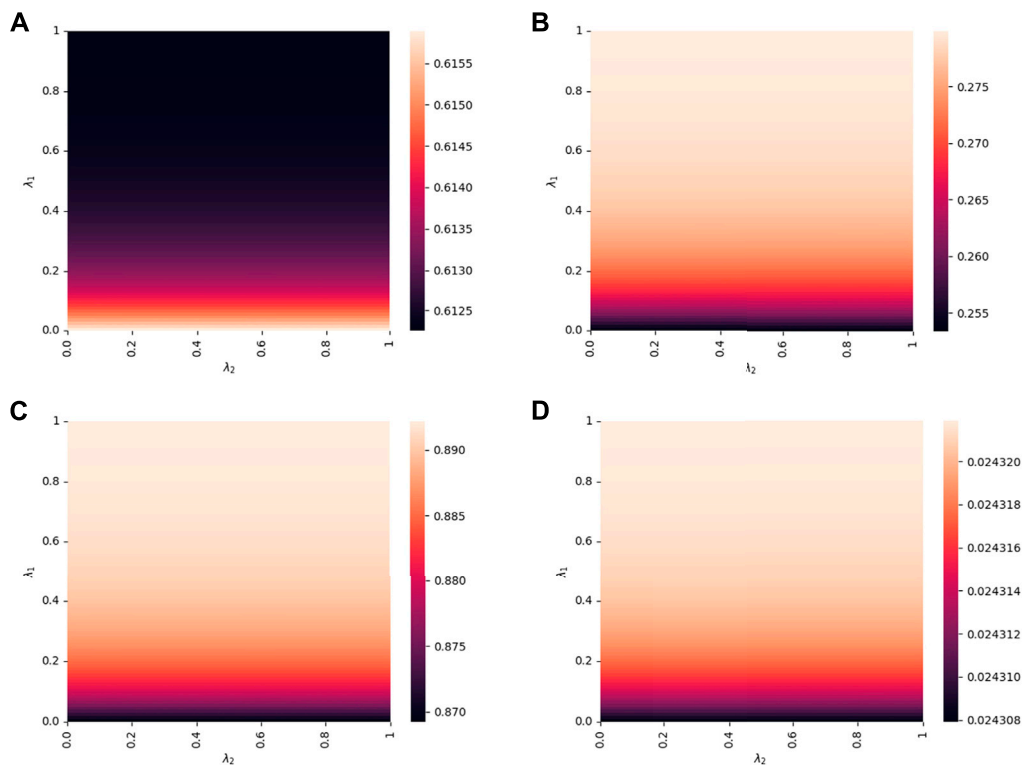


FIGURE 8

Proportions of $\rho^{A_1 I}$ (A), $\rho^{A_1 S}$ (B), ρ^{A_1} (C), and β_c (D) by MMCA as functions of λ_1 and λ_2 (awareness diffusion rate for positive and negative preventive information, respectively). The proportions get larger when the color varies from dark to light. Each heat map consists of 100×100 lattice points. Other parameters are the same as the default values.

increased epidemic size. In Figure 7F, when f_1 is lower than 0.1, the epidemic threshold β_c increases obviously with the decrease of f_1 . The results indicate that positive awareness has a pronounced inhibitory effect on epidemic spreading when $f_1 \leq 0.1$.

As for λ_1 and λ_2 (the impact of awareness diffusion rate for positive and negative preventive information), Figures 8A–D present their influence on the proportion of $A_1 I$, $A_1 S$, A_1 , and β_c , respectively. As shown in Figure 8A, for the fixed λ_2 , the final epidemic size decreases with the increase of λ_1 . Also, increases in positive awareness transmission and epidemic threshold are shown in Figures 8C, D, respectively. The result can be explained that the decrease of λ_1 promotes the spread of positive awareness. Moreover, it suppresses the spread of disease for more individuals by taking preventive measures toward the disease, thus decreasing the probability of being infectious. In addition, for the fixed λ_1 , there is little influence on the epidemic spreading with the variation of λ_2 , which can be contributed to the same reason as little variation on f_2 . However, the results do not indicate that the negative awareness-related parameters (e. g. λ_2 , f_2) have little impact on the interplay between epidemics spreading and awareness diffusion under

all conditions. In “Supplementary Material S1”, we reset the default values of parameters and incorporate additional simulations to investigate the role of negative awareness-related parameters. In general, based on our model assumption, promoting the diffusion of positive preventive information can help suppress epidemic spreading as well as the epidemic outbreak.

Effect of heterogeneity of aware individuals' states

Apart from multi-type information, heterogeneity of aware individuals' states (health state and information type) which contributes to different aware transmission capacities is also considered. In the information network, aware neighbors with different health states or different awareness states play different roles in awareness diffusion. ρ_1 , ρ_2 , and ρ_3 are proposed, representing the importance degree of aware neighbors in $A_1 S$, $A_1 I$, and $A_2 S$, respectively. Figure 9 shows the impact of ρ_1 , ρ_2 , and ρ_3 on $\rho^{A_1 I}$, $\rho^{A_1 S}$, ρ^{A_1} , and β_c . It should be noted that the “relative growth rate” is the relative difference rate compared

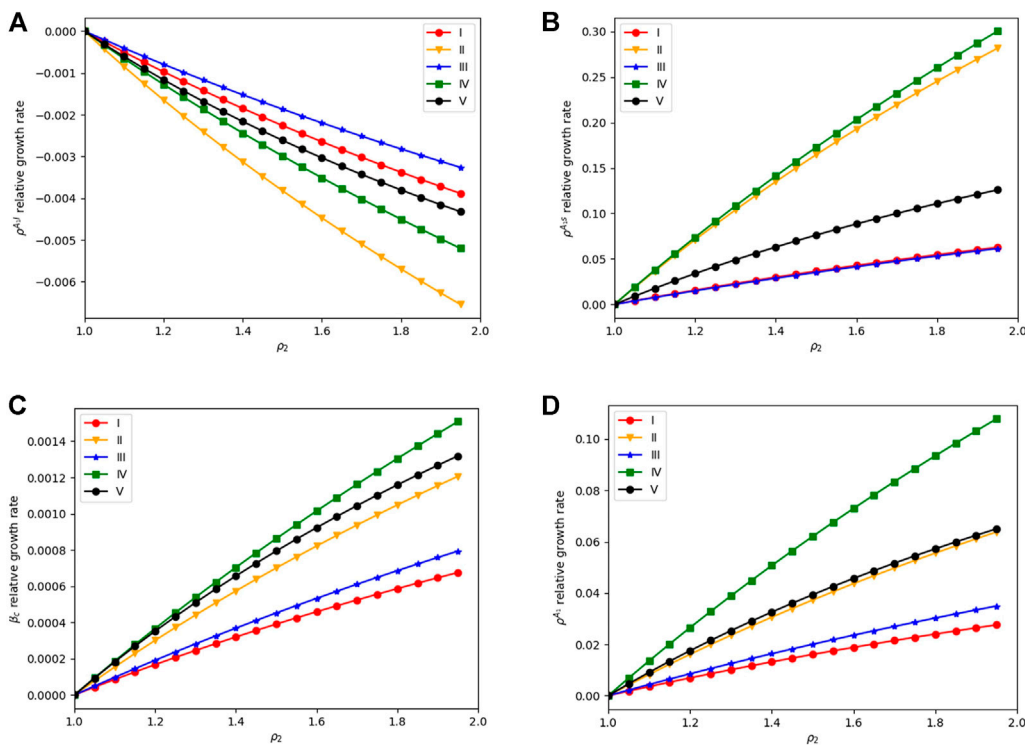


FIGURE 9
 ρ_1 , ρ_2 , and ρ_3 as functions of ρ^{A1I} (A), ρ^{A1S} (B), ρ^{A1} (C), and β_c (D). ρ_1 , ρ_2 , and ρ_3 meet the equality constraint $\rho_1 + \rho_2 + \rho_3 = 3$. I to V are results obtained with different parameter settings. (I) $\lambda_1 = \lambda_2 = 0.1$, $\delta_1 = \delta_2 = 0.3$, $\beta = 0.1$, $\mu = 0.5$; (II) $\lambda_1 = \lambda_2 = 0.1$, $\delta_1 = \delta_2 = 0.8$, $\beta = 0.1$, $\mu = 0.5$; (III) $\lambda_1 = \lambda_2 = 0.1$, $\delta_1 = \delta_2 = 0.3$, $\beta = 0.1$, $\mu = 0.7$; (IV) $\lambda_1 = \lambda_2 = 0.1$, $\delta_1 = \delta_2 = 0.8$, $\beta = 0.1$, $\mu = 0.8$; and (V) $\lambda_1 = \lambda_2 = 0.3$, $\delta_1 = \delta_2 = 0.8$, $\beta = 0.1$, $\mu = 0.8$. Also, $\rho_1 = 1$ is set for conditions I to V (Supplementary material Table S2).

with the result obtained from the basic condition ($\rho_1 = \rho_2 = \rho_3 = 1$). The basic condition represents the case that the aware neighbors are equally important and share the same information spreading rate. Results show that with the increase of ρ_2 , ρ^{A1I} decreases while ρ^{A1S} , ρ^{A1} , and β_c increase. In addition, we find that the proportions vary greatly with the increase of ρ_2 in case IV, which indicates that the importance ratios ρ_2 and ρ_3 play important roles in epidemic spreading when the recovery rate (μ) and forgotten rate (δ_1 and δ_2) are relatively large. This can be explained that, in this case, few individuals are aware of epidemics, and promoting the importance of aware neighbors can affect the coupled awareness-epidemic dynamics obviously. Compared with case IV, the proportion in case V has a lower increase. The reason is that with the increase of λ_1 (λ_2), the influence of λ_1 (λ_2) on the dynamics of epidemic spreading overwhelm the importance ratio ρ_1 , ρ_2 , and ρ_3 . Similarly, the proportion in case II also has a lower increase than that in case IV, which indicates that with the increase of forgotten rate (μ), the dynamic of epidemic spreading could be more sensitive to heterogeneity in the information diffusion.

Moreover, we also study the result with a higher infection rate (β). However, the variations of ρ_2 and ρ_3 have little impact on

the awareness-disease dynamics in such cases. Therefore, for epidemics with low infectivity (β is small), the importance ratio related to the heterogeneity of information diffusion can have an obvious impact on disease dynamics. To be specific, promoting the importance of A_1I neighbors in awareness diffusion while reducing the importance of A_2S neighbors can help suppress the epidemic spreading, especially when the recovery rate (μ) and forgotten rate (δ_1 and δ_2) are relatively large. On the contrary, for epidemics that are highly infectious like SARS or COVID-19, the influence of heterogeneity on the importance ratio of awareness neighbors is limited, making little difference for controlling epidemics.

Effect of heterogeneity of the individual degree

Another aspect of individual heterogeneity taken into account in the proposed model is the individual degree. In the physical layer, infected neighbors with different node degrees have different disease transmissibility. Factor $1 - e^{-k_j I} \sum_k$ is introduced, representing the capacity of spreading virus of the

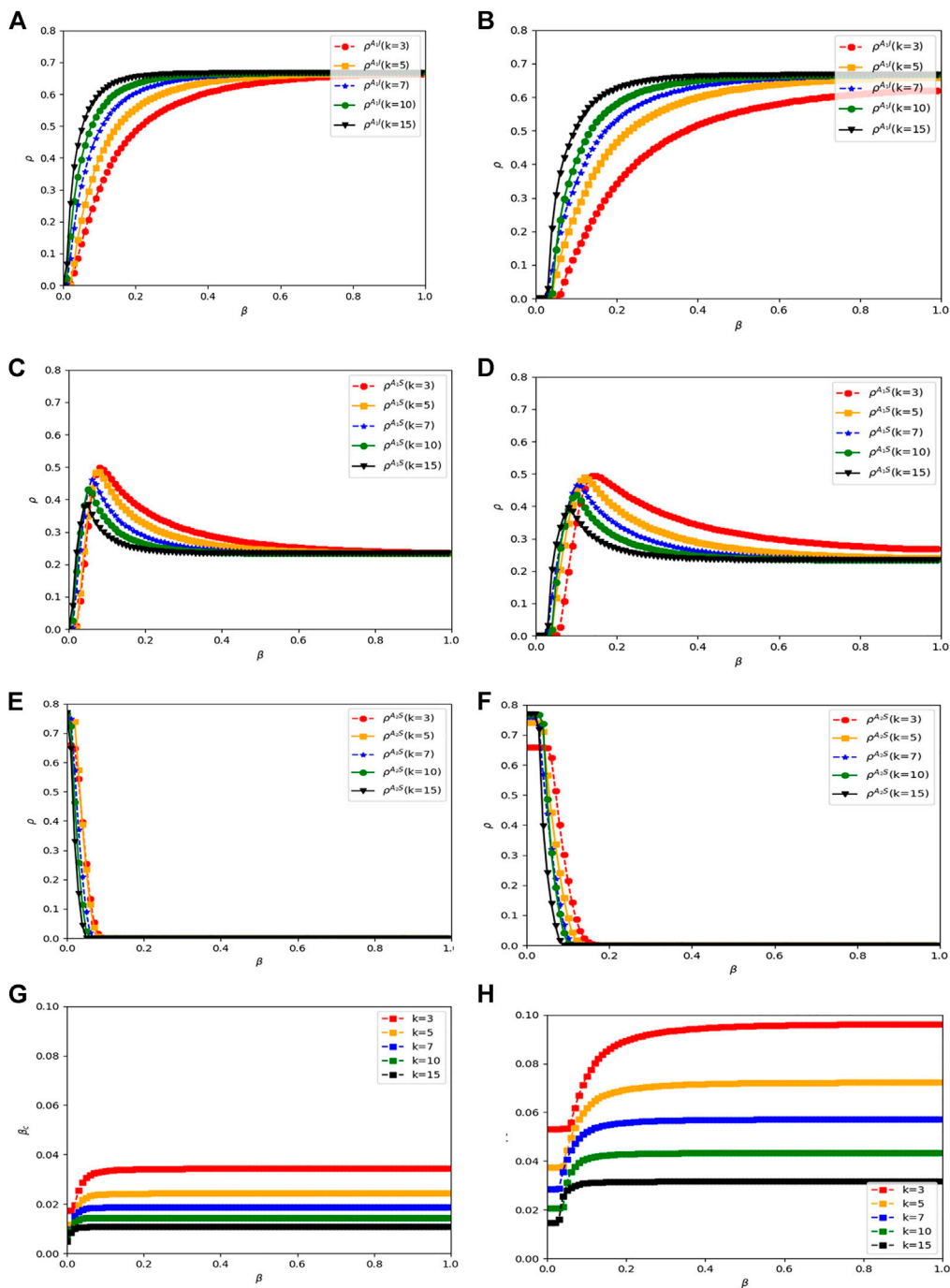


FIGURE 10
 $\rho^{A,I}$ (A,B), $\rho^{A,S}$ (C,D), $\rho^{A_2,S}$ (E,F), and β_c (G,H) as functions of β with the different node degree and different network structure. (A,C,E,G) are based on the ER-BA network (the upper layer and the lower layer are BA and ER networks, respectively), and (B,D,F,H) are based on the ER-ER network (both the upper and lower layer are the ER network). Other parameters are the same as the default values.

infected neighbor j . Figure 10 and Figure 8 present $\rho^{A,I}$, $\rho^{A_1,S}$, $\rho^{A_2,S}$, and β_c as functions of β with different node degree (k) and different network structure. Also, the subfigures on the left side (Figures 10A, C, E, G) are the results based on the ER-BA

network (the upper layer and lower layer are BA and ER networks, respectively) and the subfigures on the right side (Figures 10B, D, F, H) are the results based on the ER-ER network (both the upper and lower layers are the ER

network). In terms of the results based on the ER-BA network, with a fixed β , the proportion of infected individuals increases with the increase of average node degree (k). The differences of ρ^{A_1I} among these five cases increase when $\beta \leq 0.15$; however, when β becomes larger ($\beta \geq 0.15$), gaps among these cases become narrow. When β is close to 1, the gaps become neglectable. This phenomenon can be explained by two aspects: 1) with the increase of average node degree (k), the infected individuals can have a large range of daily activities and are more likely to transmit the virus to their neighbors, resulting in a larger epidemic size. 2) When the infection rate (β) is at a low level, the node degree plays an essential role in the dynamics of epidemic spreading. However, with the further increase of β , the impact of increasing the node degree would fade. That is, when the epidemic is highly infectious, the degree of connectivity does not play a dominant role in the epidemic spreading.

Comparing the results obtained from the ER-BA network with the results obtained from the ER-ER network, the trends for ρ^{A_1I} , ρ^{A_1S} , and ρ^{A_2S} with the increase of β_c are similar. However, considering the impact on the epidemic threshold β_c , the variation of β_c is obvious. The differences can be explained that the node degree distribution of the BA network is not uniform; once those hub nodes become infected, their high probability of infection raises the severity of their neighbors perceiving infectious disease and further leads to a severe outbreak. Therefore with the increase of average node degree, the number of hub nodes also raises up, resulting in a lower β_c . In general, a network with a low node degree can help slow down the spread of disease, and the final epidemic size is also related to the network structure. It is possible to suppress the epidemic spreading by increasing individual's social distance during the outbreak.

Conclusion

In this article, we propose an individual-based epidemics and multi-type information spreading (IEMIS) model, mainly considering two factors that can significantly affect the coupled awareness-epidemic spreading but have been rarely studied. The first factor is the multi-type information. The second factor is the individual heterogeneity (including the heterogeneity in awareness diffusion and the heterogeneity in epidemic spreading). Based on MMCA, we give out the analytical epidemic threshold of the proposed model and analyze the impact of information type and individual heterogeneity on the interplay between awareness and epidemic. The results show that the diffusion of positive awareness can help to suppress the epidemic spreading, while the influence of negative awareness is limited for the high proportion of infections leading to an overwhelming propagation of positive information. As for individual heterogeneity, enhancing the importance ratios of aware neighbors who receive positive information can elevate positive awareness spreading and further promote epidemic prevalence. Moreover, lowering the

average node degree can effectively suppress epidemic propagation, that is, cutting back social activities or increasing social distances can help control the disease.

Data availability statement

The original contributions presented in the study are included in the article/Supplementary Material; further inquiries can be directed to the corresponding author.

Author contributions

PC, XG, ZJ, and SL contributed to the methodology development and the investigation. LL and JY contributed to funding acquisition. PC and XG contributed to software, formal analysis, and the results presented in this manuscript. YH, YL, and WF contributed to supervision and validation. All authors contributed to the manuscript preparation, review, and editing.

Funding

This work was supported by the Ningbo “2025 S and T Megaprojects” [grant number 2021Z021].

Conflict of interest

Authors ZJ, SL, LL, and JY were employed by Yidu Cloud (Beijing) Technology Co., Ltd.

The remaining authors declare that the research was conducted in the absence of any commercial or financial relationships that could be construed as a potential conflict of interest.

Publisher's note

All claims expressed in this article are solely those of the authors and do not necessarily represent those of their affiliated organizations, or those of the publisher, the editors, and the reviewers. Any product that may be evaluated in this article, or claim that may be made by its manufacturer, is not guaranteed or endorsed by the publisher.

Supplementary material

The Supplementary Material for this article can be found online at: <https://www.frontiersin.org/articles/10.3389/fphy.2022.964883/full#supplementary-material>

References

- Morens D, Folkers G, Fauci A. The challenge of emerging and re-emerging infectious diseases. *Nature* (2004) 430:242–9. doi:10.1038/nature02759
- Ferguson N. Capturing human behaviour. *Nature* (2007) 446:733. doi:10.1038/446733a
- Wang Z, Andrews MA, Wu Z-X, Wang L, Bauch CT. Coupled disease-behavior dynamics on complex networks: a review. *Phys Life Rev* (2015) 15:1–29. doi:10.1016/j.plrev.2015.07.006
- Funk S, Salathe M, Jansen VAA. Modelling the influence of human behaviour on the spread of infectious diseases: a review. *J R Soc Interf* (2010) 7:1247–56. doi:10.1098/rsif.2010.0142
- Funk S, Gilad E, Jansen VAA. Endemic disease, awareness, and local behavioural response. *J Theor Biol* (2010) 264:501–9. doi:10.1016/j.jtbi.2010.02.032
- Ruan Z, Tang M, Liu Z. Epidemic spreading with information-driven vaccination. *Phys Rev E* (2012) 86:036117. doi:10.1103/physreve.86.036117
- Arefin MR, Masaki T, Kabir KMA, Tanimoto J. Interplay between cost and effectiveness in influenza vaccine uptake: a vaccination game approach. *Proc R Soc A* (2019) 475:20190608. doi:10.1098/rspa.2019.0608
- Kabir KMA, Tanimoto J. Modelling and analysing the coexistence of dual dilemmas in the proactive vaccination game and retroactive treatment game in epidemic viral dynamics. *Proc R Soc A* (2019) 475:20190484. doi:10.1098/rspa.2019.0484
- Nadini M, Rizzo A, Porfiri M. Epidemic spreading in temporal and adaptive networks with static backbone. *IEEE Trans Netw Sci Eng* (2020) 7:549–61. doi:10.1109/tNSE.2018.2885483
- Hota AR, Sundaram S. Game-theoretic vaccination against networked SIS epidemics and impacts of human decision-making. *IEEE Trans Control Netw Syst* (2019) 6:1461–72. doi:10.1109/tcms.2019.2897904
- Li X-J, Li X. Perception effect in evolutionary vaccination game under prospect-theoretic approach. *IEEE Trans Comput Soc Syst* (2020) 7:329–38. doi:10.1109/tcss.2019.2960818
- Wang H, Ma C, Chen H-S, Zhang H-F. Effects of asymptomatic infection and self-initiated awareness on the coupled disease-awareness dynamics in multiplex networks. *Appl Math Comput* (2021) 400:126084. doi:10.1016/j.amc.2021.126084
- Jia M, Li X, Ding L. Epidemic spreading with awareness on multi-layer activity-driven networks. *Physica A: Stat Mech its Appl* (2021) 579:126119. doi:10.1016/j.physa.2021.126119
- Guo H, Wang Z, Sun S, Xia C. Interplay between epidemic spread and information diffusion on two-layered networks with partial mapping. *Phys Lett A* (2021) 398:127282. doi:10.1016/j.physleta.2021.127282
- Zhan X-X, Liu C, Sun G-Q, Zhang Z-K. Epidemic dynamics on information-driven adaptive networks. *Chaos Solitons Fractals* (2018) 108:196–204. doi:10.1016/j.chaos.2018.02.010
- Wang W, Tang M, Yang H, Do Y, Lai Y-C, Lee G, et al. Asymmetrically interacting spreading dynamics on complex layered networks. *Sci Rep* (2014) 4: 5097. doi:10.1038/srep05097
- Wang W, Liu Q-H, Cai S-M, Tang M, Braunstein LA, Stanley HE, et al. Suppressing disease spreading by using information diffusion on multiplex networks. *Sci Rep* (2016) 6:29259. doi:10.1038/srep29259
- Kabir KMA, Kuga K, Tanimoto J. Analysis of SIR epidemic model with information spreading of awareness. *Chaos Solitons Fractals* (2019) 119:118–25. doi:10.1016/j.chaos.2018.12.017
- Xia C, Wang Z, Zheng C, Guo Q, Shi Y, Dehmer M, et al. A new coupled disease-awareness spreading model with mass media on multiplex networks. *Inf Sci* (2019) 471:185–200. doi:10.1016/j.ins.2018.08.050
- Guo Q, Lei Y, Jiang X, Ma Y, Huo G, Zheng Z, et al. Epidemic spreading with activity-driven awareness diffusion on multiplex network. *Chaos* (2016) 26:043110. doi:10.1063/1.4947420
- Li C, Zhang Y, Li X. Epidemic threshold in temporal multiplex networks with individual layer preference. *IEEE Trans Netw Sci Eng* (2021) 8:814–24. doi:10.1109/tNSE.2021.3055352
- Kabir KMA, Kuga K, Tanimoto J. The impact of information spreading on epidemic vaccination game dynamics in a heterogeneous complex network—A theoretical approach. *Chaos Solitons Fractals* (2020) 132:109548. doi:10.1016/j.chaos.2019.109548
- Depoux A, Martin S, Karafillakis E, Preet R, Wilder-Smith A, Larson H, et al. The pandemic of social media panic travels faster than the COVID-19 outbreak. *J Trav Med* (2020) 27:taaa031. doi:10.1093/jtm/taaa031
- Ahmad AR, Murad HR. The impact of social media on panic during the COVID-19 pandemic in Iraqi Kurdistan: Online questionnaire study. *J Med Internet Res* (2020) 22:e19556. doi:10.2196/19556
- Parveen M, Yeasmin M, Molla MMA. Antimicrobial resistance, evidences on irrational anti-microbial prescribing and consumption during covid-19 pandemic and possible mitigation strategies: A Bangladesh perspective (2020). medRxiv. doi:10.1101/2020.10.09.20210377
- Teovanovic P, Lukic P, Zupan Z, Lazic A, Ninkovic M, Zezelj I, et al. Irrational beliefs differentially predict adherence to guidelines and pseudoscientific practices during the COVID-19 pandemic. *Appl Cogn Psychol* (2021) 35:486–96. doi:10.1002/acp.3770
- Arafat SY, Kar SK, Menon V, Kaliamoorthy C, Mukherjee S, Alradie-Mohamed A, et al. Panic buying: An insight from the content analysis of media reports during Covid-19 pandemic. *Neurol Psychiatry Brain Res* (2020) 37:100–3. doi:10.1016/j.npbr.2020.07.002
- Zhang Y, Lu X, Cui N, Tang J, Zhang X. Coevolving dynamics between epidemic and information spreading considering the dependence between vigilance and awareness prevalence. *Complexity* (2021) 2021:1–13. doi:10.1155/2021/5515549
- Wang Z, Xia C, Chen Z, Chen G. Epidemic propagation with positive and negative preventive information in multiplex networks. *IEEE Trans Cybern* (2021) 51:1454–62. doi:10.1109/tcyb.2019.2960605
- Liu Q-H, Wang W, Tang M, Zhang H-F. Impacts of complex behavioral responses on asymmetric interacting spreading dynamics in multiplex networks. *Sci Rep* (2016) 6:25617. doi:10.1038/srep25617
- Guo Q, Jiang X, Lei Y, Li M, Ma Y, Zheng Z, et al. Two-stage effects of awareness cascade on epidemic spreading in multiplex networks. *Phys Rev E* (2015) 91:012822. doi:10.1103/physreve.91.012822
- Zhang H-F, Xie J-R, Tang M, Lai Y-C. Suppression of epidemic spreading in complex networks by local information based behavioral responses. *Chaos* (2014) 24:043106. doi:10.1063/1.4896333
- Guo Q, Lei Y, Xia C, Guo L, Jiang X, Zheng Z, et al. The role of node heterogeneity in the coupled spreading of epidemics and awareness. *PLoS One* (2016) 11:e0161037. doi:10.1371/journal.pone.0161037
- Chen X, Gong K, Wang R, Cai S, Wang W. Effects of heterogeneous self-protection awareness on resource-epidemic coevolution dynamics. *Appl Math Comput* (2020) 385:125428. doi:10.1016/j.amc.2020.125428
- Pan Y, Yan Z. The impact of individual heterogeneity on the coupled awareness-epidemic dynamics in multiplex networks. *Chaos* (2018) 28:063123. doi:10.1063/1.5000280
- Lyubartsev AP, Martsinovski AA, Shevkunov SV, Vorontsov-Velyaminov PN. New approach to Monte Carlo calculation of the free energy: Method of expanded ensembles. *J Chem Phys* (1992) 96:1776–83. doi:10.1063/1.462133
- Erdős P, Rényi A. *On the Evolution of random graphs*, 5. Budapest, Pest, Hungary: Publication of the Mathematical Institute of the Hungarian Academy of Sciences (1960). p. 1776–83.
- Barabasi A, Albert R. Emergence of scaling in random networks. *Science* (1999) 286:509–12. doi:10.1126/science.286.5439.509